

Cosmetic powder suspensions in compliant, fingerprintlike contacts

K. Timm

Beiersdorf AG, Research & Development, Unnastraße 48, 20245 Hamburg, Germany and Angewandte Physikalische Chemie, Universität Heidelberg, Im Neuenheimer Feld 253, Heidelberg, Germany

C. Myant^{a)} and H. A. Spikes

Tribology Group, Department of Mechanical Engineering, Imperial College London, London SW7 2AZ, United Kingdom

M. Schneider

Institut für Mikrostrukturtechnik, Karlsruher Institut für Technologie, Hermann-von-Helmholtz-Platz 1, 76344 Eggenstein-Leopoldshafen, Germany

T. Lادنorg

Institut für Funktionelle Grenzflächen, Karlsruher Institut für Technologie, Hermann-von-Helmholtz-Platz 1, 76344 Eggenstein-Leopoldshafen, Germany

M. Grunze

Angewandte Physikalische Chemie, Universität Heidelberg, Im Neuenheimer Feld 253, Heidelberg, Germany

(Received 8 July 2011; accepted 29 August 2011; published 20 September 2011)

Cosmetic powders are regularly employed in skin creams and cosmetic formulations to improve performance and enhance skin feel. A previous study investigated the effect of particle concentration and size on the lubricating properties of powder suspensions in smooth, compliant contacts [Timm *et al.*, Tribol. Int. (2011)]. In this paper the tribological properties of cosmetic powder suspensions are investigated in compliant contacts having model fingerprintlike surface topography. Friction coefficients were measured for a series of powder suspensions with varying particle size and concentration in a polydimethylsiloxane (PDMS)/PDMS contact. A commercial tribometer (MTM, PCS Instruments) was employed to measure friction as a function of rubbing time (20 min), under pure sliding (50 mm/s) and low load (0.5 N) conditions. Compared to results using smooth surfaces, it was clear that surface topography has a pronounced affect on the time-dependent tribological behavior of the cosmetic powder suspensions studied. A two-stage friction coefficient versus time curve was observed. By varying the particle size and concentration it was shown that the duration and magnitude of each stage can be controlled. © 2011 American Vacuum Society. [DOI: 10.1116/1.3640042]

I. INTRODUCTION

Polymer particles are known to influence the sensory properties of cosmetic and pharmaceutical formulations. They are believed to reduce the tackiness of skin creams and to leave a soft and powdery finish on the skin. A wide variety of powder-containing cosmetics are available and understanding the behavior of powder particles on skin would provide guidance to developers of skin-care products.

Friction has been shown to affect skin feel,¹⁻⁶ and thus the sensory performance of skin-care products. In a previous study,⁷ particulate lubricants were investigated under conditions resembling a cosmetic application. An *in vitro* system was set up using a ball-on-disk tribometer with a compliant contact formed between a smooth polydimethylsiloxane (PDMS) ball and disk. PDMS was chosen to resemble the mechanical properties of skin. The frictional behavior of polymer particle suspensions in an aqueous medium were studied in this tribometer. It was shown that the particles strongly influenced their suspensions' lubricating properties

under partially lubricated conditions, where only a small amount of lubricant was applied to the disk at the beginning of the friction test. In these tests a three-stage friction coefficient curve was observed:

Stage 1; initial low friction, corresponding to fully flooded conditions,

Stage 2; a transition period where friction rises rapidly with rubbing time,

Stage 3; friction coefficient levels out at a constant, relatively high value.

It was found that the properties of the particle suspensions can significantly influence friction in compliant contacts. The duration and magnitude of each stage in the friction plots varied with the particle size and concentration. This was because frictional behavior was highly dependent on the movement of the particles and their distribution on the contacting surfaces.

In the current study, the tribological contact has been further adapted to match the topography of human skin. Since skin-care products are applied with the consumer's fingers, tests were carried out on modified PDMS disks with grooves similar to those present on a human fingertip. The objective was to investigate the affect of this fingerprintlike structure

^{a)}Author to whom correspondence should be addressed; electronic mail: connor.myant@imperial.ac.uk

on the suspensions' lubricating properties. The change in topography is expected to affect the particle distribution and contact entrainment and thus, based on earlier work, the friction.

II. MATERIALS AND METHODS

A. Friction tests

1. Contacting surfaces

The term skin is rather vague as it is, in reality, a complex multilayered structure with viscoelastic properties. The mechanical properties of skin vary with depth. The outermost layer, the stratum corneum, is a hard layer of dead keratinized cells with a reported Young's modulus as high as ~ 1 GPa.⁸ However, the stratum corneum is only $10\text{--}40\ \mu\text{m}$ in thickness and too thin compared to the overall thickness of skin to influence the global mechanical properties.^{8,9} The stratum corneum is also likely to be broken, and possibly removed, during the application of the cosmetic creams. The innermost layer is termed the hypodermis or subcutaneous fat, which is a thick (dependent on body zone and lifestyle) soft, highly viscous, tissue. The combination of this multilayered structure is to create a low effective Young's modulus. A model skin material should be selected to represent the sub-surface bulk properties. The wetting characteristics and mechanical properties of PDMS lie within this selection criteria.

The tribological contact of interest was formed between a PDMS or nylon ball and PDMS disk. PDMS balls and disks were fabricated from a silicone kit (Sylgard 184, Dow Corning Corporation, USA). Sylgard 184 is supplied as a two part silicone elastomer kit. These two parts, base and a curing agent, were used at a mass ratio of 10:1 for all PDMS samples. The Young's modulus and Poisson's ratio of the PDMS test specimens were 2.7 MPa and 0.49, respectively. This Young's modulus lies within the range of reported elasticity for human skin of $1\text{--}4$ MPa.¹⁰ The surfaces of skin and PDMS are both hydrophobic. Water droplet contact angles were measured (OCA 20, Data Physics Instruments GmbH, Filderstadt, Germany) and found to be 95° and 110° for skin and PDMS, respectively. An MTM nylon ball (PCS-Instruments, UK) was used in one test and representative values of Young's modulus of 2.65 GPa and Poisson's ratio 0.39 were employed for calculations using this material.¹¹

Surface roughness values for the PDMS and nylon balls were obtained using an optical profilometer (Veeco Instruments Inc, Plainview, NY). Measurements were taken in the vertical scanning interferometry mode and the camera was set up with an $\times 20$ objective lens. Images were 640×450 pixels, which equates to a field of view of $\sim 575 \times 430\ \mu\text{m}$. No filtering was used during measurements. Root-mean-square roughness values of 501 ± 20 and 650 ± 50 nm were measured for the PDMS and nylon balls, respectively.

Fingerprint-textured PDMS disks having a fine pattern of radial grooves were prepared using a mold. Disk groove geometry was based on real fingerprints. Fingerprints from the right hand index finger of five test persons were measured using a phase-shifting rapid *in vivo* measurement technique,

PRIMOS (GfK Messtechnik, Teltow, Germany).^{12,13} Dimensions of the fingertip grooves were found to vary considerably from person to person and from groove to groove; therefore average dimensions of groove width $350\ \mu\text{m}$ and groove depth and spacing $300\ \mu\text{m}$ in the test region were used. These precise dimensions were also constrained by the dimensions of the micromechanical tools used to make the primary, positive molds. Initially, a metallic positive mold having radial grooves was made by micromechanical machining. This was then used as a template to produce polysulphonate molds via a hot embossing process. These molds were negatives, with radial ridges in place of grooves. Finally, PDMS was cast into these molds and hardened to produce replicas of the original positive. A PDMS disk and an SEM image of its grooves are shown in Figs. 1(a) and 1(b), respectively. Figure 1(c) shows a schematic drawing of the groove dimensions at the tested radius on the disks.

2. Experimental procedure

Friction measurements were carried out using a minitraction machine (MTM; PCS Instruments, London, UK). A compliant contact was obtained by loading a molded 9.5 mm diameter PDMS ball against the flat surface of a molded, textured PDMS disk. A detailed description of the experimental procedure is given in Ref. 7.

For each test, the PDMS disk and ball were cleaned with de-ionized water and isopropanol and left to dry in air. For partially lubricated conditions, $25\ \mu\text{l}$ of test lubricant were applied dropwise using an Eppendorf pipette (Eppendorf AG, Hamburg, Germany) and immediately spread via the operator's finger covered with a sterile finger glove (AMPri GmbH, Stelle, Germany), resembling a cosmetic application. Tests were carried out under conditions similar to those experienced during descriptive skin cream panel testing.

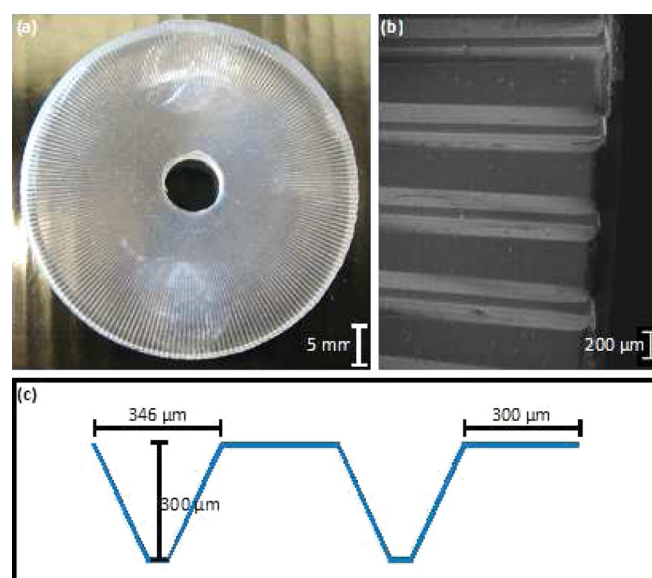


FIG. 1. (Color online) (a) Photograph of a structured PDMS disk; (b) SEM image of the grooves; (c) schematic drawing of the groove dimensions in the middle of the ball track on the disk which is located 2 mm from the disk edge.

Measurements were conducted in an air conditioned room to ensure a relatively constant temperature ($18 \pm 2^\circ\text{C}$) and humidity ($43 \pm 3\%$). An applied load of 0.5 N was employed and the tests were performed under pure sliding conditions at a disk speed of 50 mm/s. All tests were conducted for 20 min and repeated at least twice; average values are depicted in the plots showing friction coefficients versus rubbing time. The test period was chosen to correspond to the sensory panel testing which employs a rubbing time of 5 min, at $\sim 37^\circ\text{C}$. The longer laboratory test period was due to the reduced absorption and evaporation rates of the suspension medium.

3. Images of the contact region and estimation of the number of particles in the contact

Since it was not possible to visualize the contact interface during sliding, some friction tests were stopped after different rubbing times and the PDMS samples removed from the test apparatus. Images of the contact area on ball and disk were then taken using a color CCD-camera and microscope setup with a $5\times$ magnification lens. Due to the large contact size, multiple images of the contact were captured and then stitched together. The total number of particles present within the contact was estimated from these images; only particles on the elevated areas were counted. This was carried out in order to gain insights about the distribution of particles at different stages during the sliding tests.

B. Cosmetic powders and test lubricants

1. Particle size

Nylon 12 particles (Arkema, Colombes, France) were used as supplied. Particle size distribution was determined using a Mastersizer 2000 (Malvern Instruments Ltd., Malvern, UK), at least twice per sample. Polydispersity is expressed by the span according to British Standards [BS 2955]. The particle size distributions of the three different nylon powders used in this study were found to be 11.5 ± 0.6 , 21.8 ± 0.6 , and $63.2 \pm 0.6 \mu\text{m}$ (mean diameter \pm span).

2. Test lubricants

The aqueous suspension medium (SM) and the preparation of test suspensions have been described in detail previously.⁷ In addition to water and cosmetic particles, each lubricant contained a rheology modifier (Carbopol 980; 0.1 wt. %) and an emulsifier (Polysorbate 20; 1 wt. %). The powder content was varied between 0 and 30 wt. %.

Rheological properties of the samples were determined using an AR-G2 rheometer (TA Instruments, Philadelphia) under ambient conditions (25°C). Across the shear rate range tested (10^{-1} – 10^4 s^{-1}), the SM and all the powder suspensions were found to be shear-thinning. All had high shear rate viscosity in the range ~ 0.01 – 0.06 Pa s .

C. Adhesion between nylon particles

The force of adhesion between nylon particles of $21.8 \mu\text{m}$ diameter was determined with an atomic force microscope

[(AFM), MFP-3D BIO, Asylum Research, Mannheim, Germany]. Particles were glued to a microscope slide using adhesive tape.^{14,15} Single particles were fixed at the ends of tipless AFM cantilevers (Tipless-All-In-One-AI; NanoAnd-More GmbH, Wetzlar, Germany). To do this, a cantilever was fixed to the underside of a holder attached to the xyz-object stage of a microscope. The cantilever was first moved with the microscope stage to a drop of epoxy resin. By moving the end of the cantilever into the resin a small amount of resin was transferred onto the cantilever. Finally, a particle was picked up with the cantilever. In this way the particles could be precisely positioned and glued to the end of AFM cantilevers.¹⁵ Once this process was completed the AFM cantilevers were transferred to the AFM and employed for interparticulate adhesion measurements.

Force–distance curves were obtained using the AFM. During the unloading stage, adhesive forces between the surface and the AFM tip hinder the retraction of the tip and a pull-off force is observed from which adhesive forces can be determined. The same loading rate was employed for all measurements at 0.2 Hz, which equates to a separation speed of 400 nm/s.

III. RESULTS

A. Effect of suspended particles on friction

To obtain reference behavior, friction tests in the absence of particles were conducted first. These enable the specific contribution of the particles to friction to be identified.

Friction coefficient versus time was recorded under dry conditions (when no lubricant is added) and for the contact lubricated by the aqueous SM without particles. $25 \mu\text{l}$ of the SM were spread on the disk prior to testing. Further tests were then carried out with a suspension of nylon particles of diameter $21.8 \mu\text{m}$ and a concentration 30 wt. %. The resultant friction behavior is shown in Fig. 2.

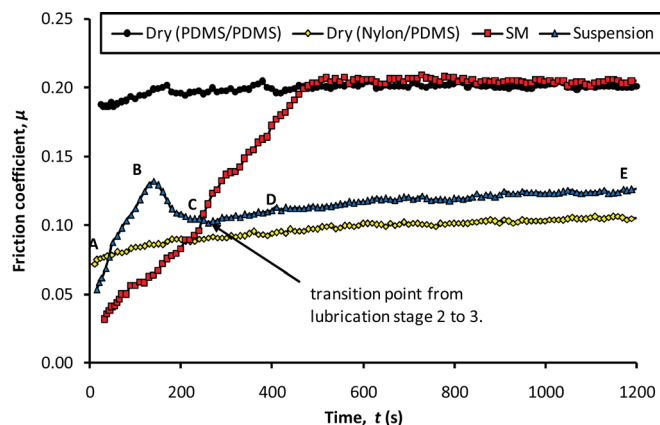


FIG. 2. (Color online) Friction coefficients vs time for PDMS/PDMS under dry conditions (black circles), lubricated by SM only (red squares) and a nylon suspension $21.8 \mu\text{m}$ 30 wt. % (blue triangles). Also shown is the result for a nylon ball on PDMS disk under dry conditions (yellow diamonds). (a)–(e) Stages where separate tests were halted and photomicrographs of the contact taken, as discussed.

For the unlubricated contact, a constant, relatively high friction coefficient of ~ 0.20 is observed. When the contact is lubricated by the SM a clear reduction in the initial friction is observed. Friction then rises immediately until, after ~ 500 s, it levels out at a similar value to the dry contact.

When lubricated with a suspension a striking effect on friction is observed. Unlike with tests using smooth disks,⁷ there is no initial constant low friction region, referred to in previous work as stage 1. Only the two subsequent stages of behavior, seen using particulate suspensions with smooth disks, are observed with textured disks. For consistency with the work on smooth disks these are referred to as stages 2 and 3. In the first part of the friction curve (stage 2), friction rises rapidly to reach a spike, peaking at $\mu = 0.13$, followed by a decrease to a value of $\mu = 0.10$. From this point onwards (stage 3) the friction slowly rises for the duration of the test, to reach a level roughly half that of the dry contact test. This behavior was repeatable in multiple tests.

Also presented in Fig. 2 is the friction trace from an unlubricated test where a PDMS disk was rubbed against a nylon ball instead of a PDMS ball. This was conducted to identify any differences in friction between PDMS on PDMS and nylon on PDMS. The result shows that friction coefficient is ~ 2 times lower for a nylon/PDMS contact compared to a PDMS/PDMS contact. This suggests that, in principle, if nylon particles wholly support the load in a PDMS/PDMS contact, friction should be reduced from the high PDMS/PDMS value to one approaching the much lower nylon/PDMS value.

To help explain the characteristics of the friction curve for the particle suspension, images of the disk were taken from different duration tests which illustrate the distribution of particles in and around the contact area. These are presented in Fig. 3. Figures 3(a)–3(e) represent the stages of the curve shown in Fig. 2 corresponding to $t = 0, 150, 200, 400, 1200$ s, respectively.

At the beginning of the test, the elevated areas of the structured disk are covered with particles, while very few are visible within the grooves [Fig. 3(a)]. After ~ 150 s [Fig. 3(b)], when the friction coefficient peaks, very few particles can be seen on the elevated areas on the disk (or in the contact region of the ball). Instead, particles accumulate in the grooves. After $\sim t = 200$ s, individual particles can be seen

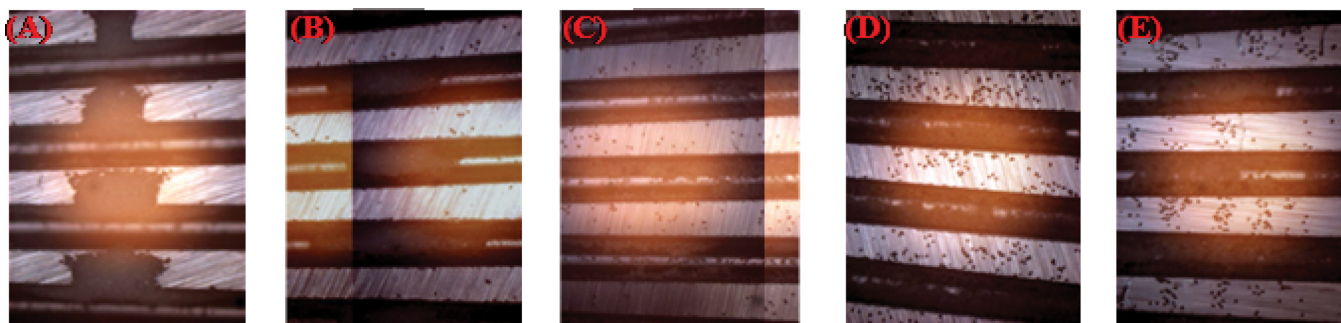


FIG. 3. (Color online) Images of the tribological contact of interest. (a)–(e) Stages of the curve shown in Fig. 2. Elevated areas appear in light gray while particles and grooves appear dark. Contact inlet is at the top for all images.

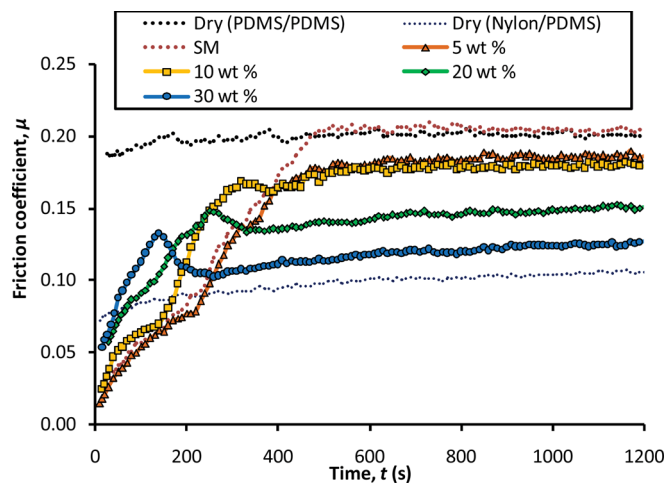


FIG. 4. (Color online) Plots of friction coefficients vs time for the tribological contact lubricated with suspensions of $21.8 \mu\text{m}$ diameter nylon particles at various concentrations. Dotted lines: The plots from Fig. 2 for the dry contact and for the contact lubricated by the SM only.

on the elevated areas [Fig. 3(c)]. Over the remainder of the test a small increase in particle numbers on the elevated areas can be seen, leveling out with time [Figs. 3(d) and 3(e)].

B. Effect of particle concentration and size

To determine the influence of particle concentration on friction, five different concentrations were tested, all with $21.8 \mu\text{m}$ diameter particles. Figure 4 shows the effect of particle concentration on the friction coefficient over the test period. The particle-free plots from Fig. 2 are shown as dotted lines.

It is important to note that all the concentrations of the suspensions are in weight percent. Therefore, increasing particle concentration will result in a decrease in the volume of SM in the applied test lubricant.

The effect of increasing particle concentration is to increase the initial friction coefficient, at $t = 0$ s, and decrease the duration and magnitude of stage 2 while also making stage 2 more pronounced. Concentration appears to have negligible effect on the rate of increase in friction

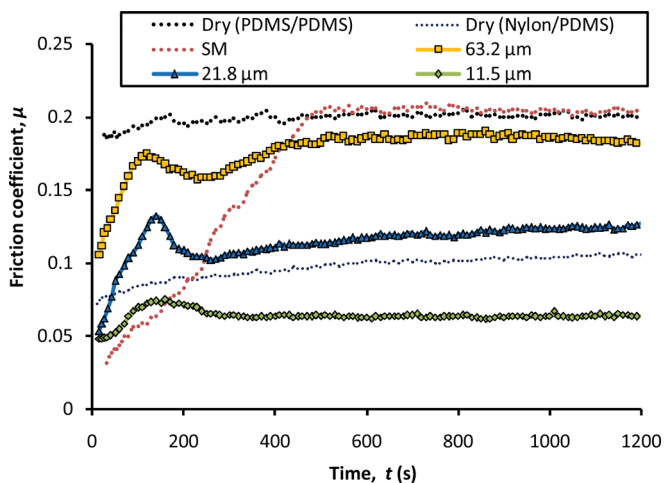


Fig. 5. (Color online) Plots of friction coefficients vs time for the tribological contact lubricated with suspensions of nylon particle suspensions of different size, all at 30 wt. % concentration. Dotted lines: The plots from Fig. 2 for the dry contact and for the contact lubricated by the SM only.

coefficient during stage 3, but there is a clear decrease in magnitude of friction coefficient with increasing particle concentration.

Figure 5 shows the effect of particle size on friction coefficient over the test period. All suspensions used were at 30 wt. % concentration, while mean particle diameters were 11.5, 21.8, and 63.2 μm . As mentioned earlier, it is important to remember that all suspensions were produced by weight percent. Therefore, increasing particle size will result in a decrease in particle number. However, unlike particle concentration, varying particle size should result in the same SM volume for all tests.

Particle size appears to have negligible effect on the duration of both stages. However, a clear relationship between particle size and the magnitude of friction in each stage is observed, with increasing particle size giving higher friction. With increasing particle size, stage 2 becomes more pronounced. No obvious increase in friction occurs during stage 3 for 11.5 μm diameter particles, while a steady increase is observed for 21.8 μm diameter particles. For the largest particles (63.2 μm) a rapid increase is seen at the start of stage 3; after ~ 150 s a plateau is reached, before a slight decrease in the final ~ 400 s of the test.

Photomicrographs of the contact region, captured at the end of each test, showed that very few particles of 63.2 μm diameter were left in the tribological contact. In contrast, a large number of particles of 11.5 μm diameter were still visible on both disk track and ball contact region.

C. Skin feel of powder suspensions

A trained, descriptive panel evaluated the suspensions' skin feel 5 min after application, according to the SpectrumTM method.¹⁶ The panel reported that suspensions of higher powder concentration and smaller particles exhibit a more "powdery" skin feel.

IV. DISCUSSION

A. Friction between dry surfaces

The total friction coefficient, μ_{tot} , in unlubricated, dry contacts can be described as the sum of an interfacial adhesion term, μ_{int} , and a deformation term, μ_{def} . The interfacial adhesion term corresponds to the energy dissipated in the rupture of intermittent junctions formed between the two sliding surfaces due to short-range molecular attractive forces, such as van der Waals interactions. This equates to the real area of contact, A , multiplied by the interfacial shear stress, S ($\mu_{\text{int}} = SA$). In order to apply this model to skin, both A and S must be identified. There are a number of ways of describing the origins of the interfacial shear stress for elastomeric materials, including a reversible peeling (adhesive) process involving the propagation of Schallamach waves.¹⁷ However, prediction of the interfacial shear stress is complex, requires detailed material property data, and was beyond the scope of this project.

The deformation component μ_{def} arises from the incomplete recovery of the energy dissipated by subsurface viscoelastic deformation within the contact. For a dry pure sliding contact, the value for μ_{def} is much lower than the total friction coefficient,⁷ which shows the overwhelming importance of interfacial adhesion in dry contacts.

For one experiment, presented in Fig. 2, the PDMS ball on the MTM was replaced with a nylon one. A significant reduction in the overall friction coefficient was observed. This may be due to lower adhesion between nylon and PDMS compared to PDMS on PDMS, but may also be due to a difference in mechanical properties. The stiffer contact and smaller contact area will reduce the deformation component, but as for the PDMS/PDMS contact, the contribution to the total friction from deformation will still be small compared to the adhesive contribution.

In a previous paper,⁷ the friction coefficient for an unlubricated smooth PDMS/PDMS contact (under the same conditions employed in this study) was reported to be ~ 0.44 . The introduction of a fingerprintlike topography lowers this to almost half, ~ 0.2 . It is likely that a lowering in the real contact area is responsible for this lower friction coefficient, as the interfacial shear stress is the same in both cases. However, for an unlubricated smooth nylon/PDMS contact (under the same conditions employed in this study), friction was reported to have a similar value to that reported here, ~ 0.08 . If there were a direct relationship between the total friction and real contact area, one would expect a lowering in the friction coefficient for the nylon/PDMS contact with the introduction of a fingerprintlike topography. It may be that any lowering in the interfacial component is offset by an increase in the deformation losses, which due to the grooved surface structure of the PDMS disk are now complex and difficult to predict analytically. However, such a large increase in the deformation losses seems unlikely. Instead, it is possible that in the PDMS/PDMS contact, the elastic flattening was not enough to achieve full conformity within the grooves since some considerable deformation of the ball

occurred. When the stiffer nylon ball is employed, all the deformation will occur in the PDMS disk. Now the elastic flattening may be enough to make the real area of contact almost the same as for the, previously investigated, smooth surfaces.

B. Lubrication by SM

When the contact is partially lubricated by SM only, the initial value of the friction coefficient is low presumably because the contact is operating in the isoviscous-elastohydrodynamic regime.⁷ A steady increase in friction is then observed over the initial ~ 400 s. This results from progressive starvation due to the loss of lubricant from the contact inlet reservoir. This loss may result from either capillary flow along the disk grooves away from the contact, or evaporation of the small test lubricant volume, or both. Since a similar, though slower, increase in friction was seen for smooth surfaces, evaporation must play a part.⁷

C. Effect of particle addition

It is clear from Fig. 2 that the presence of solid particles influences each stage of the friction curve. The effect of particle size and concentration on the duration and magnitude of each stage is now discussed.

1. Stage 2: spike in friction coefficient

a. Particle cohesion. When lubricated by particle suspensions, a spike occurs in the beginning of each plot (stage 2). This spike does not appear in the absence of particles (when the tribological contact is lubricated by the SM only) or in the absence of SM (when the applied suspension is dried prior to testing). The effect of the SM on interparticle adhesion was investigated using an AFM. The average pull-off force between two nylon particles (21.8 μm diameter) was determined from ten repeats and the results are summarized in Table I. Force–distance curves recorded with an AFM indicate that the volume of liquid surrounding each particle strongly affects interparticle adhesion. When particles are fully immersed in SM, interparticle attraction is low, with a value of 35 nN. However, when the particles are damp, this value is found to increase strongly to 2000 ± 500 nN. When the particles are dry the interparticle attraction is again low. This suggests that the maximum in friction coefficient during stage 2, where fluid evaporation is known to be occurring, is controlled by interparticle interaction.

TABLE I. Interparticle adhesion expressed by the pull-off force determined with an AFM for wet, damp, and dry nylon particles.

Particle's state	Pull-off force (nN)
Fully immersed in the SM	35 ± 5
Damp	2000 ± 500
Dry	180 ± 10

For a perfectly wetting liquid bridge between spherical particles in contact with each other, the strength of the cohesive force, F_{bridge} , approaches

$$F_{\text{bridge}} = 2 \cdot \pi \cdot R_{\text{particle}} \cdot \gamma_{\text{liquid}}, \quad (1)$$

where R_{particle} is the radius of a particle and γ_{liquid} is the surface tension of the liquid.¹⁸ The surface tension of the SM was determined with the ring method at 20 °C and found to be 34.7 mN/m. Based on this, Eq. (2) predicts a value of 2.4 μN for F_{bridge} . This is in close agreement with the experimentally determined adhesion force of $2 \mu\text{N} \pm 0.5 \mu\text{N}$ using the AFM.

Kudrolli¹⁸ comments that the addition of small amounts of liquid to granular matter transforms its mechanical properties. At the beginning of each test the particulate lubricant can be considered as slurry with the interstitial space between particles fully saturated with liquid and cohesion between particles negligible. This allows the particles to move freely into the disk grooves. Due to the rapid onset of starvation, demonstrated by the very rapid rise in friction, SM volume is reduced and particles begin to form large contiguous wet clusters. As starvation continues, these clusters are no longer fully saturated with water so liquid bridges, bounded by air, are formed between adjacent particles. These bridges induce cohesion between grains, making it difficult to transport particles out of the grooves. Friction then rises due to an increase in the PDMS/PDMS contact area.

Friction continues to increase until effectively all the SM is lost, including the liquid between particles. Friction now falls from its maximum value as particles become mobile and move from the grooves to be entrained into the contact zone. Stage 2 ends when only a dry granular matter remains and friction begins to slowly rise again as there is a very slow loss of particles from the lands between the grooves.

Increased particle concentration will lead to more cohesion of the damp clusters within the grooves and this will cause fewer particles to be entrained out of the groove and into the contact. This will increase the PDMS/PDMS contact area and friction. This is represented in Fig. 4 by the more pronounced spike in stage 2. Higher particle concentrations will also lead to more rapid fluid evaporation. However, if concentration is maintained and particle size increased (Fig. 5) particle numbers will decrease, suggesting a lower overall cohesive strength of the particle clusters, and reduction of the friction spike. This; however, is not the case, as results show a more pronounced spike with increasing particle size. Perhaps with increased radius of curvature the surface tension of the liquid bridges between particles is increased greatly, although this seems unlikely. It is more reasonable to suggest that larger particles are harder to entrain and therefore fewer enter the contact. Thus, friction is greater throughout the entire test, as seen in Fig. 5.

While particle number and size appear to control the friction coefficient magnitude, the volume of SM present has an important effect on the duration of each stage. The transition

between stages 2 and 3 is controlled by the complete removal of the SM. Increased particle concentration results in a smaller SM phase volume. Therefore, removal of the SM will occur more rapidly, as shown in Fig. 4. When concentration is maintained and particle size varied, SM volume will be constant (only particle number changes) and the time taken for complete removal of the SM should be the same in all cases. This is confirmed in Fig. 5, where the duration of each stage is the same for all suspensions.

b. Particle entrainment. Wan and Spikes¹⁹ investigated the behavior of suspended solid particles in rolling and sliding elasto-hydrodynamic contacts and noted that as the slide roll ratio increased (toward a pure sliding contact), more particles were trapped in the inlet. This accumulation, they noted, caused fluid starvation but was periodically pulled through the contact.

Using a free-body diagram of a single particle and the geometry of a Hertzian inlet, neglecting fluid forces and inertia, it can be seen that the force couple due to a sliding contact would tend to cause the particles to rotate, while a rolling contact would drag the particle through the contact.¹⁹ Dwyer-Joyce²⁰ showed, through simple theoretical analysis, that the friction coefficient between the particles and main contact surfaces, as well as the particle size, determined particle entry. Larger particles require a higher friction coefficient to be entrained into the contact. This agrees with the current observations that increased particle sizes decrease particle entrainment.

Dwyer-Joyce²⁰ also observed that fluid forces build up in the inlet region and smaller particles tend to be swept around the sides of the contact. This shedding can occur at a distance from the contact center several times larger than the contact radius. Only particles on a central flow line or those large enough to be trapped between the closing surfaces pass into the contact. The motion of the particles in the inlet region is governed by the fluid motion and the drag forces acting on the particles. Only a very small volume of liquid can pass through the contact, so the majority of the liquid must either sweep around the contact or flow backwards out of the contact. Dwyer-Joyce explains that most of the fluid/particle mixture is swept around the outside of fully flooded point contacts. Thus, particles on the central streamline will be subjected to lower off-axis fluid drag forces and enter the contact, while those traveling off-axis tend to get swept around the sides of the contact.

Once the particles are in contact with both counterfaces, according to Nikas they are acted on by solid frictional forces and fluid forces.²¹ The fluid forces acting on the particles are caused by the pressure differences across the particles and the dynamic forces resulting from the obstruction of the fluid flow caused by the presence of particle accumulation in the inlet. The solid forces result from the friction between the particles and surrounding counterfaces. Nikas and Sayles²² show that the solid frictional forces are several orders of magnitude larger than the fluid forces, and the static forces are greater than the dynamic fluid forces. There-

fore, as SM is removed, more particles are likely to enter the contact due to greater entrainment forces.

The concentrating effect of the contact, which is more marked for larger particles, can be explained by particles getting trapped in the inlet region, and subject to frictional entrainment forces further from the contact, resulting in them being carried into the contact region. These frictional entrainment forces counteract the larger drag forces acting on the larger particles, which have the effect of carrying the particles around the contact. There is a maximum size of particle that can be entrained into a contact due to geometry. At higher entrainment speeds, the drag forces on the particles are increased, which results in a greater degree of contact evasion.²³

For the contact of interest the SM volume rapidly decreases. Therefore, fluid forces rapidly become negligible and then surface forces will dominate.

2. Stage 3: slow rise until test finish

Plots of friction coefficient versus time show that the friction coefficient value rises very slowly during stage 3. It is assumed that during this stage, little or no SM is left in the contact inlet reservoir. Only dry particles remain on the contact track, so that any differences in friction behavior originate only from solid particles. Plots show that the presence of particles within the contact reduces the friction coefficient compared to the unlubricated contact.

It was shown previously⁷ that the particles located within the contact reduce interfacial adhesion by reducing the real area of contact. The high friction coefficient observed for the unlubricated contact has been ascribed to strong interfacial adhesion between the PDMS surfaces. Figure 2 shows that for a pure nylon/PDMS contact, friction is greatly reduced compared to a pure PDMS/PDMS contact. The reduction is due to a change in the interfacial adhesion. Interfacial adhesion is proportional to the real contact area and the interfacial shear stress and the introduction of the nylon particles will reduce both.

Figure 6 shows the friction coefficients, recorded at the end of each test, plotted versus the measured percentage of the contact region between ball and disk covered by particles. The percentage of the contact covered by particles was estimated from the particle size and the number of particles counted in the contact region on the disk at the end of each test. Figure 6 clearly shows that with increasing particle concentration or decreasing particle size, a greater area of the contact region is covered by the nylon particles, that smaller particles are easier to entrain, and increased concentration improves entrainment probability. Increased particle number within the contact increases the nylon/PDMS area, resulting in a lowering of the friction coefficient.

Figure 6 shows an inverse linear relationship between the friction coefficient and the disk track area covered with particles. It is interesting to note that the final friction coefficient for a nylon/PDMS contact, Fig. 2, was ~ 0.09 , which is

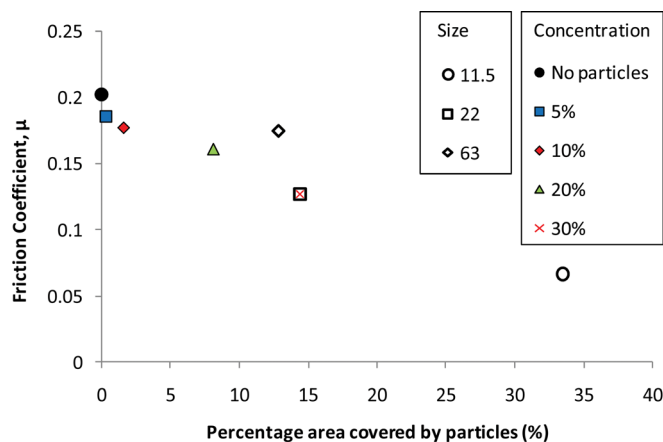


FIG. 6. (Color online) Friction coefficients recorded at the end of various tests with suspensions of nylon particles vs percentage of disk track covered by particles. Variations in size were at a fixed concentration of 30 wt. %, while variations in concentration were for one particle size of 21.8 μm .

somewhat larger than the result for the smallest particles, $\mu = 0.05$. The likely explanation is a smaller overall real contact area for the latter. To find the true relationship between particle size and concentration on the final friction coefficient, the real contact area must be known.

D. Lubricating properties and skin feel of powder suspensions

The results of these friction tests were then compared to perceived skin feel after application of powder suspensions. The latter was assessed by a trained, descriptive panel. Since talcum powder has been shown to reduce friction in compliant contacts²⁴ and on skin,^{25–28} low friction coefficient values are expected to correspond to “powdery” skin feel.

Temperature of volar forearm skin is reported to be around 32 °C (Refs. 10, 29, and 30) and is therefore higher than the temperature of the above-mentioned friction tests. Also, unlike the PDMS surfaces used for the friction tests, the skin absorbs water. Therefore, only the final friction coefficient values, where the aqueous SM has fully evaporated, will be of interest for comparison with the perceived skin feel measurements.

In contrast to experiments on smooth disks,⁷ the final friction coefficient value obtained on the structured disks in this study varies with particle concentration and is lower for suspensions with higher initial particle concentration. Assuming that low friction corresponds to powdery skin feel, these results are in accordance with panelist evaluations. Possibly, the grooves on a human fingertip also act as reservoirs for the powder, releasing it after the evaporation of the aqueous suspension medium, like the grooves on the structured PDMS disks. Images taken of the fingertip after application of a powder suspension show clearly that particles are, indeed, located in the grooves; Fig. 7 shows an example. The decrease in final friction coefficient value with decreasing particle size is in accordance with the more powdery skin feel as assessed by the descriptive panel.

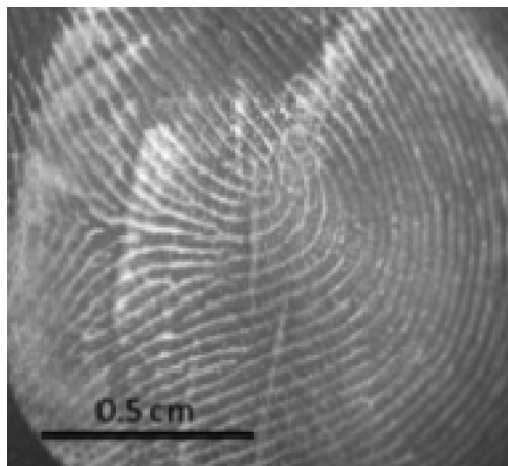


FIG. 7. Photograph of a fingertip after application of a powder suspension.

V. CONCLUSIONS

The lubricating properties of cosmetic powder suspensions, in a fingerprintlike contact, were investigated using a ball-on-disk tribometer. Tests were conducted at room temperature for 20 min at a constant sliding speed of 50 mm/s. The real contact area and therefore, friction, was shown to decrease with increasing particle entry. Particle contact entry was dependent on particle size and concentration. The volume of SM was also found to influence particle entry by controlling interparticulate cohesion.

Particles were observed to move from the elevated areas on the disk into the grooves immediately after sliding commenced. As SM was lost, cohesion between the particles increased until a critical SM volume was reached, at which point cohesion decreases. This was represented as a spike in friction plots and is termed “stage 2.” Upon drying, interparticle adhesion became negligible and particles could be entrained into the contact with little difficulty. From this point on friction behavior entered “stage 3.” There was little change in friction over the remaining test period. Grooves are believed to promote the initial loss of fluid phase and then act as reservoirs, “feeding” the contact with particles and helping to maintain a relatively low friction coefficient.

Increased particle size and concentration produced a more pronounced friction spike in stage 2. However, opposing effects were observed for stage 3. Increased particle concentration caused friction to decrease, while increased particle size caused increased friction.

The impact of suspended particles on friction measured in this study correlate well with perceived skin feel panel tests and the use of test disks with texture based on fingerprint morphology is essential for this correlation. This suggests that the test method described in this study, as well as providing fundamental information about the behavior of particles in compliant contacts and their impact on friction, may also be of use in the development of personal care products.

ACKNOWLEDGMENTS

The authors wish to thank Nils Hoffmann and Margaret Horton (Beiersdorf AG) for inspiring discussions, Henrike

Nuguid (Beiersdorf AG) and the panelists for describing the sensory perception after application of various powder suspensions, Thorsten Bretschneider (Beiersdorf AG) for support with PRIMOS, and Matthias Worgull (KIT) for his support in preparing the fingerprinted molds. The authors are grateful to the Arkema group for supplying nylon particles and to Beiersdorf research for permission to publish results.

- ¹E. L. Cussler, S. J. Zlotnick, and M. C. Shaw, *Percept. Psychophys.* **21**, 504 (1977).
- ²J. K. Prall, *J. Soc. Cosmet. Chem.* **24**, 693 (1973).
- ³H. Tanimoto and M. Nashimoto, *Cosmet. Toiletries* **94**, 20 (1979).
- ⁴S. Nacht, J. A. Close, D. Yeung, and E. H. Gans, *J. Soc. Cosmet. Chem.* **32**, 55 (1981).
- ⁵M. Lodén, H. Olsson, L. Skare, and T. Axéll, *J. Soc. Cosmet. Chem.* **43**, 13 (1992).
- ⁶X. Liu, Z. Yue, Z. Cai, D. G. Chetwynd, and S. T. Smith, *Meas. Sci. Technol.* **19**, 1 (2008).
- ⁷K. Timm, C. Myant, H. A. Spikes, and M. Grunze, *Tribol. Int.* (2011).
- ⁸C. Pailler-Mattei, S. Pavan, R. Vargiolu, F. Pirot, F. Falson, and H. Zahouani, *Wear* **263**, 1038 (2007).
- ⁹Y. Yuan and R. Verma, *Colloids Surf., B* **48**, 6 (2006).
- ¹⁰P. Agache and P. Humbert, *Measuring the Skin* (Springer, Berlin, 2004).
- ¹¹W. D. Callister, *Materials Science and Engineering. An Introduction* (Wiley, New York, 2000).
- ¹²U. Jacobi, M. Chen, G. Frankowski, R. Sinkgraven, M. Hund, B. Rzany, W. Sterry, and J. Lademann, *Skin Res. Technol.* **10**, 207 (2004).
- ¹³S. Jaspers, H. Hopermann, G. Saueremann, U. Hoppe, R. Lunderstädt, and J. Ennen, *Skin Res. Technol.* **5**, 195 (1999).
- ¹⁴L.-O. Heim, J. Blum, M. Preuss, and H.-J. Butt, *Phys. Rev. Lett.* **83**, 3328 (1999).
- ¹⁵M. Preuss and H.-J. Butt, *Langmuir*. **14**, 3164 (1998).
- ¹⁶M. Meilgaard, G. V. Civil, and B. T. Carr, *Sensory Evaluation Techniques*, 3rd ed. (CRC Press, London, 1999).
- ¹⁷S. A. Johnson, D. M. Gorman, M. J. Adams, and B. J. Briscoe, *Tribol. Ser.* **25**, 663 (1993).
- ¹⁸A. Kudrolli, *Nature Mater.* **7**, 174 (2008).
- ¹⁹G. T. Y. Wan and H. A. Spikes, *Tribol. Trans.* **31**, 12 (1988).
- ²⁰R. S. Dwyer-Joyce, *The Effects of Lubricant Contamination in Rolling Element Performance* (University of London Press, London, 1993).
- ²¹G. K. Nikas, *J. Tribol.* **124**, 461 (2002).
- ²²G. K. Nikas and R. S. Sayles, *Proc. Inst. Mech. Eng., Part J: J. Eng. Tribol.* **212**, 333 (1998).
- ²³R. S. Dwyer-Joyce, *Wear* **233-235**, 692 (1999).
- ²⁴J. K. Appeldoorn and G. Barnett, *Proc. Sci. Sect. Toilet Goods Assoc.* **40**, 28 (1963).
- ²⁵S. Comaish and E. Bottoms, *Br. J. Dermatol.* **84**, 37 (1971).
- ²⁶A. F. El-Shimi, *J. Soc. Cosmet. Chem.* **28**, 37 (1977).
- ²⁷W. A. Gerrard, *Bioeng. Skin* **3**, 123 (1987).
- ²⁸P. F. D. Naylor, *Br. J. Dermatol.* **67**, 327 (1955).
- ²⁹J. Bray, P. A. Craig, A. Macknight, R. Mills, and D. Taylor, *Lecture Notes on Human Physiology* (Blackwell Science, Oxford, 1999).
- ³⁰D. Walmsley and P. G. Wiles, *Int. J. Microcirc. Clin. Exp.* **9**, 345 (1990).